Multi-Leaf Spring and Hotchkiss Suspension

CAE Simulation

Peiyong Qin, Glenn Dentel, and Mikhail Mesh

Abstract: Leaf spring design was mainly based on simplified equations and trial-and-error methods. The simplified equation models were limited to the three-link mechanism assumption and linear beam theory.

This paper presents detailed finite element modeling and analysis of a two-stage multi-leaf spring, a leaf spring assembly, and a Hotchkiss suspension using ABAQUS. Non-linearity from large deformation, interleaf contact, and friction was included. Stresses and strains under different loads were analyzed. The spring and suspension characters such as spring rate, windup rate, roll rate, and roll steer were analyzed. Analysis results correlated well to laboratory test results.

The simulation method presented can be used for the development of leaf springs and Hotchkiss suspensions. Durability can be predicted before prototyping. Suspension characteristics can be verified after the leaf geometry is designed. In addition, the rates predicted can be used in full vehicle NVH models or multi-body dynamic models. Over all, the method introduced can help to reduce product development time and costs significantly.

1. Introduction

A Hotchkiss suspension is a solid axle suspension that is commonly used on trucks for its higher load-carrying capacity (Figure 1). The suspension consists of a solid axle, two leaf springs, two shackles, and rubber bushings. The front eyes of the springs and one end of the shackles are mounted to the truck frame through bushings. The rear eyes of the spring are connected to the other end of the shackle through bushings. The wheels are mounted at the ends of the axle. The jounce bumpers are mounted to frame.

Currently, leaf spring design mainly relies on simplified models and trial-and-error methods. The simplified models use a three-link mechanism to simulate the leaf spring's behavior (SAE, 1996, and SAE, APR80). They also use small deflection beam theory for stress calculation (Wachtel, 1987).

The development of finite element methods, especially of non-linear analysis makes it possible to study leaf springs more accurately. A literature search was done. A paper about nonlinear analysis (Liu, 1988) was found, but it only discussed mono-leaf springs. Another paper (Tavakkoli, 1996) discussed leaf spring modeling in MSC/NASTRAN and MDI/ADAMS using beam elements. It showed accurate prediction in jounce condition but not in roll condition.

The purpose of this study was to use existing leaf spring data to develop and validate detailed multi-leaf spring FEA models so that they can be used to support product development. According to assembly

procedures, three non-linear FEA models were built and studied using ABAQUS as analysis tool. They are defined as following:

- *Leaf spring*: This was the center-bolted leaf spring supported on rollers at both eyes. Bushings were not included. The bolt clamping procedure was simulated. Vertical leaf spring rate and strain data were studied.
- *Leaf spring assembly*: This was the U-bolt clamped spring with the bushings and shackle included. The assembly procedures were simulated. Suspension vertical rates, windup rates, and strain data were analyzed.
- *Full suspension*: This was the complete rear Hotchkiss suspension. Roll rate and roll steer were studied. The extreme cornering case was also analyzed.

2. Model

2.1 Leaf spring

Separate leaves were modeled in solid elements based on CMM (Coordinate Measuring Machine) measured geometry (Figure 2). They were then put together along the center-bolt hole. The nylon tip inserts were modeled as solid elements. The zinc interleaves between leaves were ignored because they were too thin to model and have small effects on spring behaviors.

Contact pairs of leaf-tip-insert-to-leaf and leaf-middle-to-leaf-middle were defined. Friction was included in all contact pair definitions.

The model was positioned such that the x direction was from spring front eye to rear eye, z direction was vertical upward. The front eye was constrained in x, y and z translation and x and z rotation, allowing free y rotation. The rear eye was constrained in y and z translation and x and z rotation, allowing free x extension and y rotation.

The center-bolt clamp load was applied, then the assembled geometry was used to simulate the vertical push test.

The loading block used in test was modeled as rigid and connected to the forth leaf only in the vertical direction (Figure 3). Its dimensions are shown in (SAE standard, 1998). Solid element block was also used but the results did not show much difference from those of the rigid model.

2.2 Leaf spring assembly

The model generation of leaf spring assembly is shown in Figure 4(a~d). The assembly procedures are as following:

1) Each part was modeled and put together. The axle tube, clamping plate, and clamping bracket were modeled in shell elements. The U-bolts were modeled as beam elements. Each bushing was modeled as six spring elements to simulate the stiffness of six degrees of freedom. See Figure 4(a).

2) U-bolt clamp load was applied with all bushing bolts loose, i.e., the torsional stiffness (y rotation) was released by removing the corresponding spring element. The center-bolt clamp load was ignored here, because it was relatively smaller compared to U-bolt clamping and the center area was almost ‘‘dead’’ after U-bolt clamping. See Figure 4(b).

3) The axle tube was pushed upward to curb position (vehicle height position without payload, i.e., no driver, passengers, or cargo) with all three bushings loose. See Figure 4(c).

4) The bushing bolts were tightened at curb position, i.e., the spring elements for bushing torsional stiffness were activated. Then the vertical force was unloaded. See Figure 4(d).

The geometry after the last step was the assembled geometry and used for rate studies.

In all the simulations, boundary conditions used were fixed leaf-spring-front-eye bushing bolt and shackle-to-frame-bushing bolt.

2.3 Full suspension

The leaf spring assembly model in Figure 4(d) was mirrored across the vehicle to create the full suspension model. The axle tube was modeled as beam elements, except the sections above the springs. These sections were modeled in shell elements for jounce bumper contact. They were connected to the beam elements using rigid “spider”. (Refer to Figure 14).

The jounce bumper was modeled as a nonlinear spring element. Contact between the jounce bumper and the axle tube was defined. The bumper surface was modeled in shell elements for contact purpose only.

The leaf-spring-front-eye bolt and shackle-to-frame bolt were constrained in all six degrees of freedom. The frame end of jounce bumper was also constrained in all directions.

3. Analysis and results

3.1 Leaf spring vertical push

Upward load was applied in 15 steps through the loading block. The vertical displacement at the loading point was measured (Figure 3).

Strain gages were used to correlate strains between test and analysis. Gage #1 was on the top of the main leaf, close to the center. Gage #2 was on the bottom of the third leaf, near the rear end. Gage #3 was on the bottom of the forth leaf, i.e., the second stage leaf, close to the center.

The force-displacement curves of both analysis and test are plotted in Figure 5. The vertical spring rate curves were obtained by differentiating the force-displacement curves, i.e., getting the slope of the curve in Figure 5. They are shown in Figure 6. The analysis and test strain data are shown in Figure 7. From these plots, it can be seen that:

- The analysis results match very well with test results. The displacement error of analysis was within 2% relative to test. The vertical spring rate error was less than 4%.

- At the transition area of the curves, the second stage leaf was beginning to engage. Before the second-stage leaf was engaged, the spring rate was almost constant and the third strain gage reading was zero. As the second-stage leaf was gradually engaged, spring rate increased significantly. After the second-stage leaf was engaged, the spring rate still increased a little bit as load increased. This was mainly because of geometry non-linearity.

3.2 Leaf spring assembly vertical push

For the assembly vertical push study, an upward load was applied in 15 steps using the model assembled in Figure 4(d).

The force vs displacement curves are plotted in Figure 8. The vertical rate vs displacement curves are shown in Figure 9. The strain data are shown in Figure 10. The strain gage locations are the same as in the leaf spring case.

From the plots, one can see that

- The displacements and rates correlated well. Before the second-stage leaf was engaged, the vertical rate was almost constant with a little bit of decrease as load increased. Compared with a constant rate in the leaf spring vertical push case (Figure 6), shackle motion could be the reason. After the second-stage leaf was engaged, the suspension rate increased gradually as load increased.
- Before the second-stage leaf was engaged, the strain data from analysis correlated very well to those from test. After that, there was a little bit offset.

3.3 Leaf spring assembly windup

For windup study, analysis was done at two positions. On was at the curb position and the other was at a second-check-point position. The curb position is a vehicle height position when the vehicle has full fluid, but no driver, no passengers, and no cargos. The second-check-point position is a position with payload such that the second-stage leaf was just fully engaged. Fore and aft loads were applied at tire patch to obtain the windup-moment-vs-angle curves. See Figure 4(e & f).

The curves are shown in Figure 11. The slopes of the curves are the windup rates. It can be seen that the rate at the second checkpoint was higher than that at curb. This was because that the second-stage leaf was fully engaged at the second checkpoint and it was only half engaged at curb. The rate in braking was higher than that in acceleration in both cases. This was because that the leaf spring was unsymmetrical. The second-stage leaf engaged more in braking than in acceleration. In acceleration the rear tip of the second-stage leaf separated from the third leaf, but in braking, the front did not.

The twist angle of the rear spring eye bushing was obtained from analysis. The maximum relative twist was 18 degrees from curb position. It happened at braking at second checkpoint. This information can be used for bushing design.

Unfortunately, there were no test data to compare for this case.

3.4 Suspension roll

For suspension roll study, loads were applied to push the suspension to curb position. Then moment was applied to the suspension by increasing the vertical load at the left side and decreasing the load at the right side. This roll moment without a cross vehicle load was a GoodYear SPMM (Suspension Parameter Measure Machine) test condition.

Figure 12 shows the roll moment vs roll angle curve. It can be seen that the relation was about linear. The roll rate was calculated by linearly fitting the curve using least square criteria. The difference between the calculated result and the test result was only 5%. See Table 1.

Roll steer was also measured in the analysis. It was defined as wheel steering angle change due to suspension roll. The steer angle was measured as the vertical component of rotational displacement vector at the axle end (wheel center). The roll angle was measured as the overall rotation of the axle around the fore-aft direction. Wheel center fore-aft movement at different suspension heights and some elastic deformation of the axle caused steer angle change.

Figure 13 shows the steer angle vs roll angle curve of analysis. Linearly fitting the curve yields the roll steer for left wheel and right wheel (Table 1). Compared with GoodYear SPMM test results, they are acceptable.

3.5 Suspension at cornering

For cornering study, the proving ground (PG) test load, representing ballasted vehicle to GVWR (Gross Vehicle Weight Rate), was applied vertically at both sides. Each side took half of the total load. The right side was then unloaded and the left side was doubly loaded. After that, a rightward force was added to the left tire patch. The rightward load was the maximum lateral load obtained from PG. This was to simulate extreme right turn case of a loaded vehicle, i.e., when the right wheel was about to leave the ground.

The final deformed shapes and von Mises stresses were shown in Figure 14.

It can be seen that after cornering load was applied, the axle tube compressed the jounce bumper on the left side.

The maximum roll angle was about 10 degrees from analysis, close to what was observed at PG, which was about 8 degrees (Table 1). Approximate lateral force applied, or linear bushing rates used, or the less extent of cornering at PG could cause the difference.

4. Conclusions and future work

The leaf spring, leaf spring assembly, and full suspension models developed are successful. Most analysis results correlate very well with test results.

The models can be used to study:

- Leaf spring vertical rates.
- Leaf spring assembly vertical and windup rates.

- Full suspension roll rate and roll steer.
- Leaf spring durability.
- The effects of geometry, friction, bushings, shackles, clamping, pre-load, etc.

The predicted rates can also be used in full vehicle NVH (Noise, Vibration, and Harshness) models such as NASTRAN models or multi-body dynamic models such as ADAMS models.

Future work is to use the modeling and analysis techniques to develop new products or improve existing products.

5. References

1. Gillespie, T. D., "Fundamentals of Vehicle Dynamics", Society of Automotive Engineers, Inc, 1992.

2. Liu, W., "Nonlinear Analysis Theory of Single Leaf Steel Springs", SAE Paper 881744, 1988.

3. SAE, "Manual on Design and Application of Leaf Spring", SAE HS788, APR80.

4. SAE, "Spring Design Manual", SAE AE-21, 1996

5. SAE Standard, "Leaf Springs for Motor Vehicle Suspension—Made to Customary U.S. Units—SAE J510 NOV92", SAE Handbook, Vol. 2, p20.09, 1998.

6. Tavakkoli, S, Aslani, F., and Rohweder, D, "Analytical Prediction of Leaf Spring Bushing Loads Using MSC/NASTRAN and MDI/ADAMS", MSC World Users' Conference, 1996.

7. Wachtel, D. W., Adkins, D. E., May, J. M., and Hohnstadt, W. E., "Advances in the Design, Analysis, and Manufacturing of Steel Leaf Springs", SAE Paper 872256, 1987.

Table 1. Full suspension result comparison

Case	FEA	Test	Difference
Roll rate (ft.lbs/deg)	440.4	418.4	5%
Roll steer left (deg/deg)	0.0266	0.0236	11%
Roll steer right (deg/deg)	0.0337	0.0262	22%
Roll angle at extreme cornering (deg)	10	8	20%

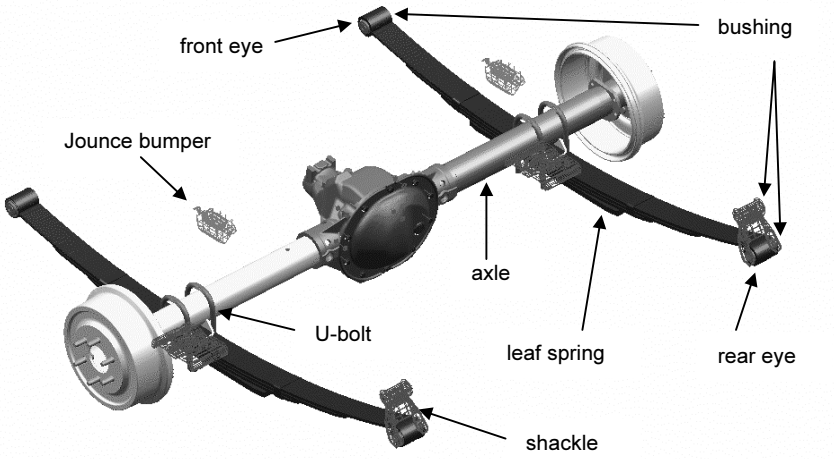

Figure 1. A Hotchkiss suspension.

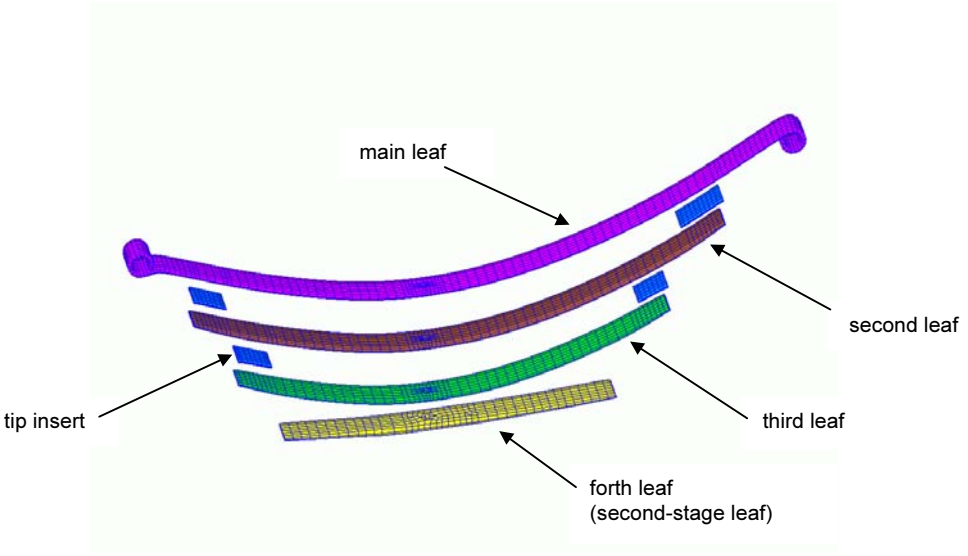

Figure 2. Leaf spring modeling.

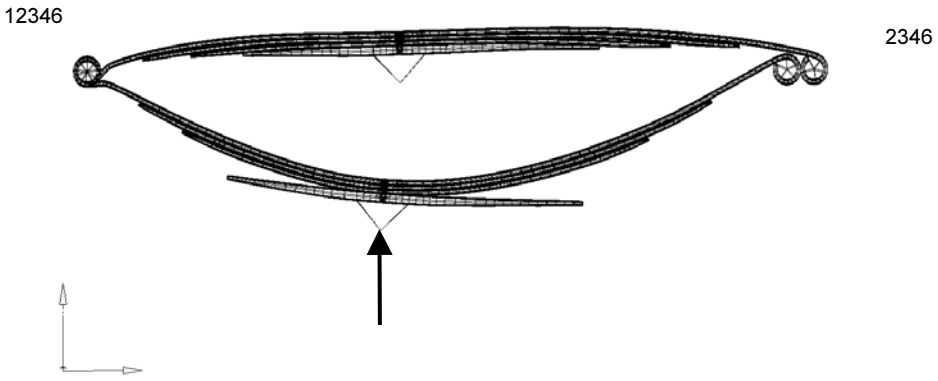

Figure 3. Leaf spring vertical push.

(a) Model before clamping

(b) U-Bolt clamping

(c) Pushing to curb w/ bushing bolts loose

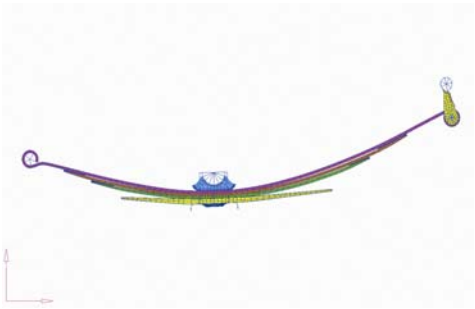

(d) Tightening bolts and unloading

(e) Braking at 2nd checkpoint

(f) Acceleration at 2nd checkpoint

Figure 4. Leaf spring assembly.

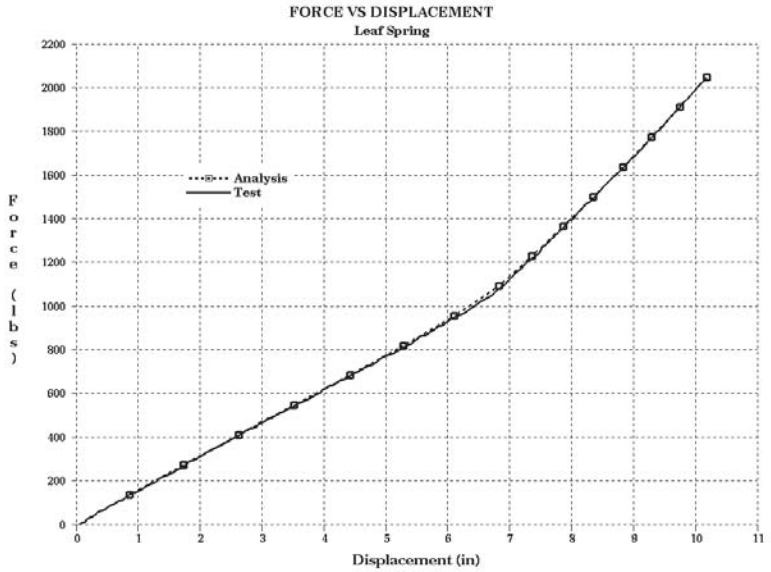

Figure 5. Force vs displacement curve of leaf spring.

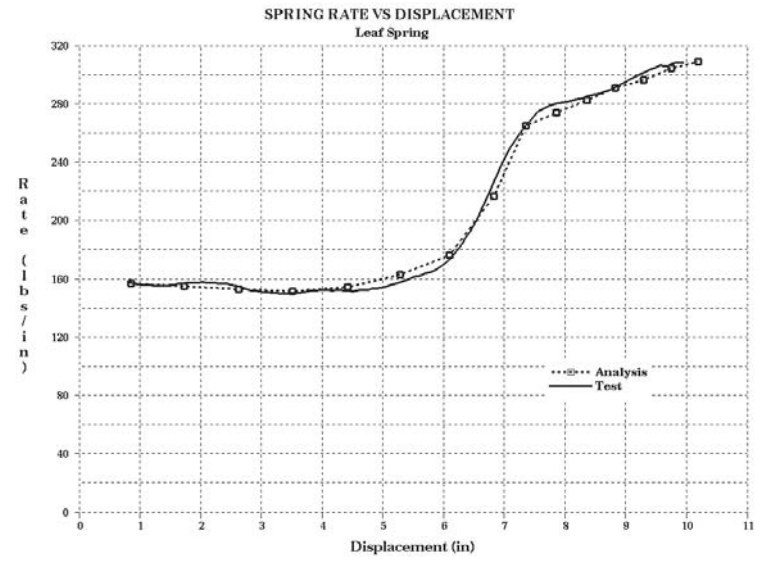

Figure 6. Spring rate vs displacement curve of leaf spring.

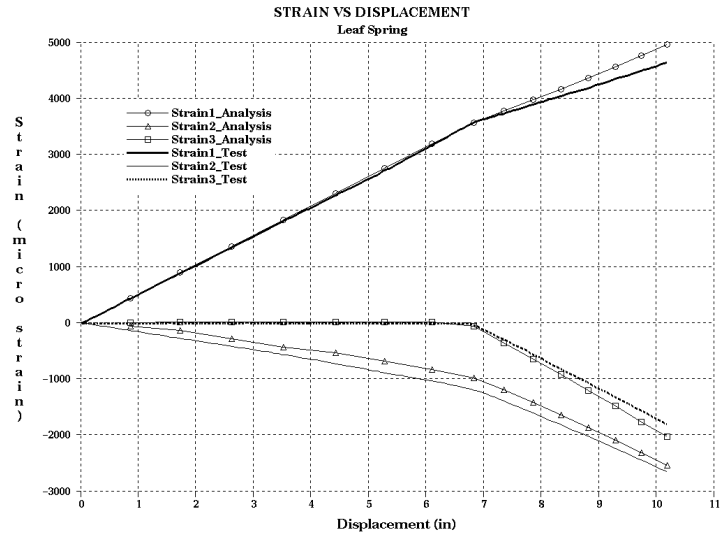

Figure 7. Strain vs displacement curves of leaf spring.

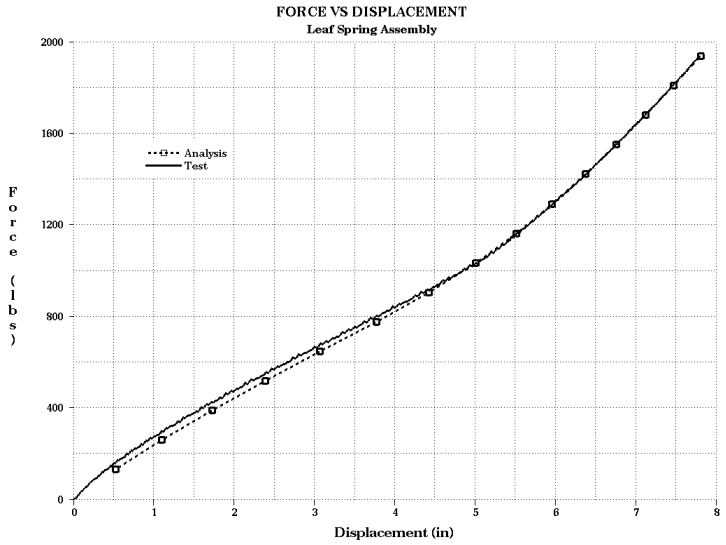

Figure 8. Force vs displacement curve of leaf spring assembly.

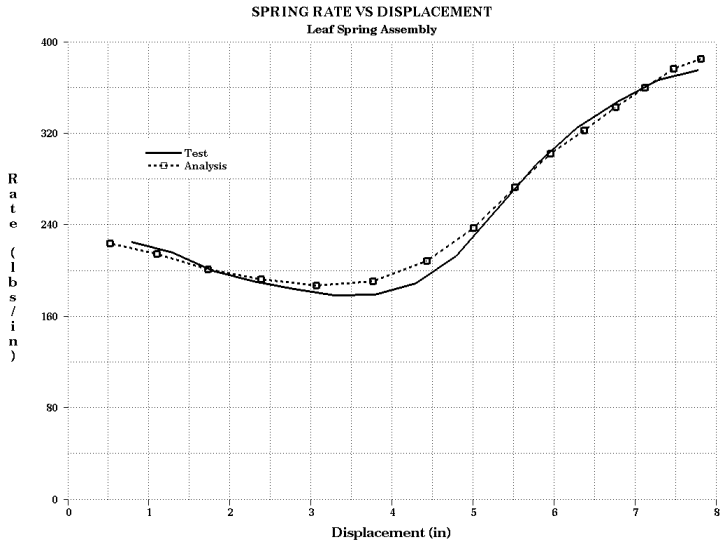

Figure 9. Vertical rate vs displacement curve of leaf spring assembly.

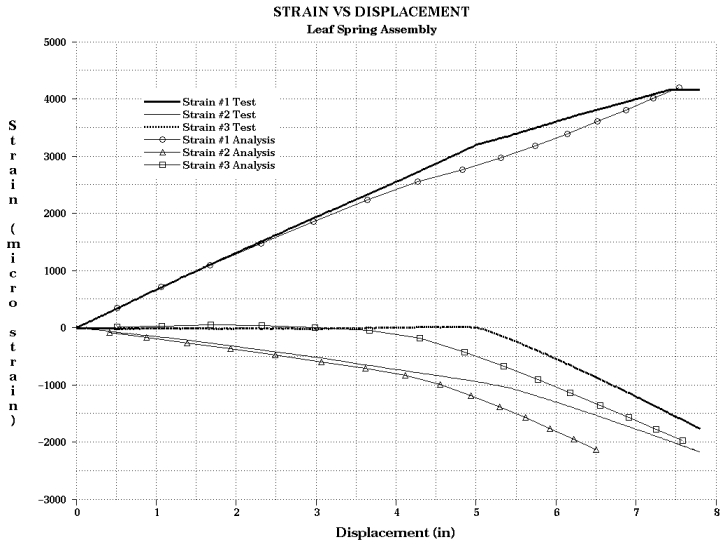

Figure 10. Strain vs displacement curves of leaf spring assembly.

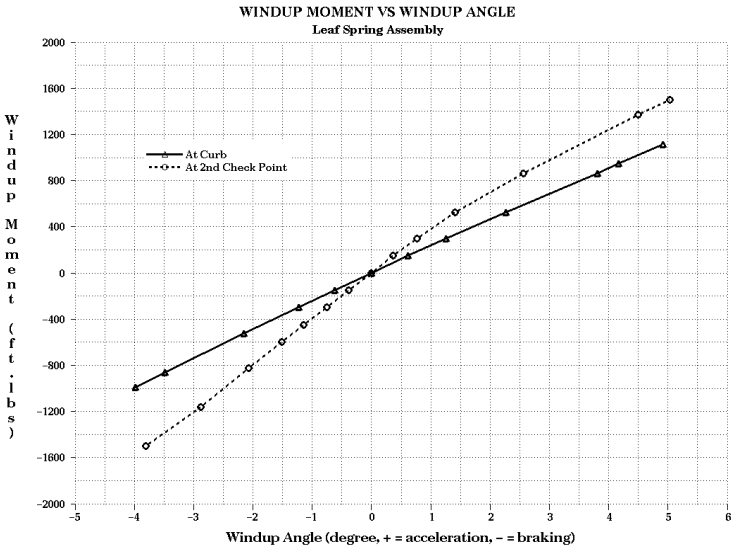

Figure 11. Windup moment vs windup angle curves of leaf spring assembly.

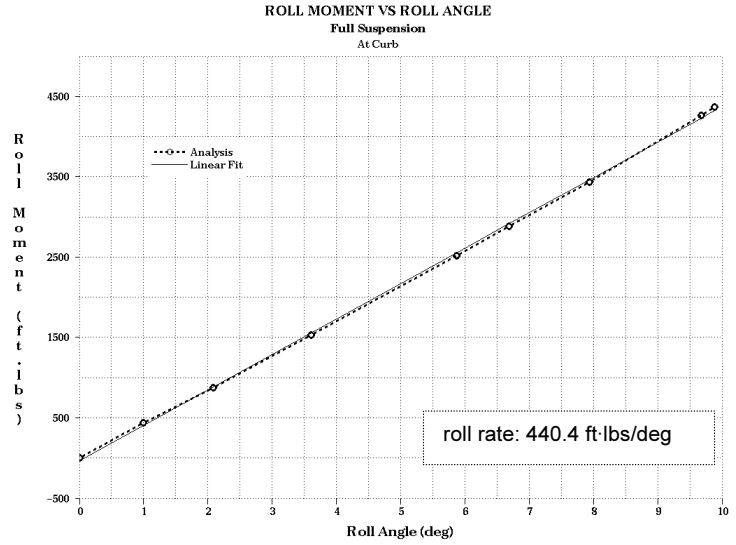

Figure 12. Roll moment vs roll angle curve of full suspension.

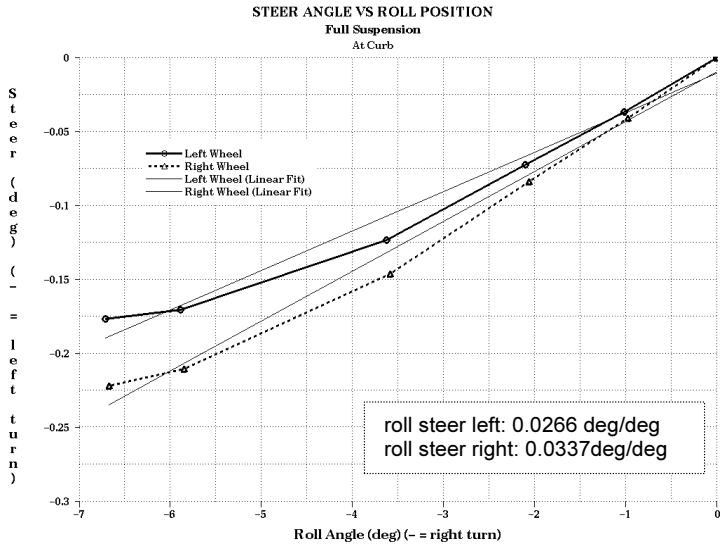

Figure 13. Steer angle vs roll angle curve of full suspension.

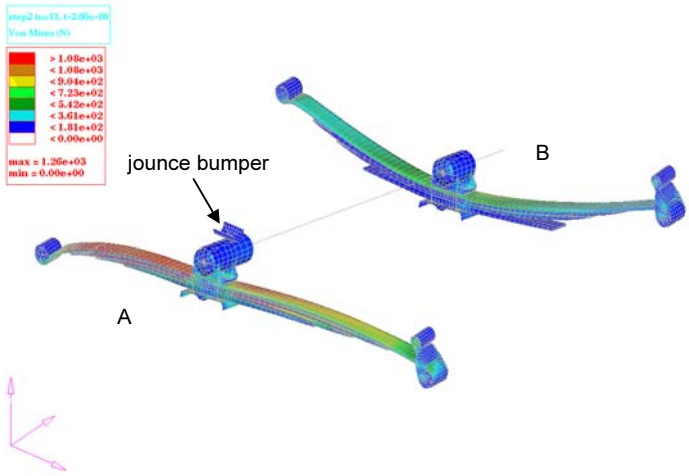

Figure 14. Deformed shape and von Mises stress (MPa) of full suspension at extreme cornering.